TABLE I
POWER LOSS PER TRANSIT FOR DOMINANT MODE BETWEEN PARALLEL STRIP MIRRORS

N	Loss $= 1 - \lvert\kappa_1\rvert^2$	
	Variational method	Iterative method
$\frac{1}{2}$	0.1639	0.1740
1	0.0607	0.0800
2	0.0217	0.0320
3	0.0108	0.0194
4	0.0080	0.0129

TABLE II
POWER LOSS PER TRANSIT FOR LOWEST ODD MODE BETWEEN PARALLEL STRIP MIRRORS

N	Loss $= 1 - \lvert\kappa_2\rvert^2$	
	Variational method	Iterative method
$\frac{1}{2}$	0.6035	0.5397
1	0.2401	0.2698
2	0.0863	0.1207
3	0.0468	0.0703
4	0.0308	0.0478

no reason for presuming that the variational values of $\lvert\kappa_1\rvert$ are better than the iterative ones because they are larger than the latter values. In this connection it is interesting to note that the variational values for $\lvert\kappa_2\rvert$ do not all lie on the same side of the iterative results.

The foregoing remarks are not intended to keep anyone from applying variational principles to integral equations with complex symmetric kernels if he so desires. One pays for the "efficiency" of the variational technique by not knowing how accurate the approximate eigenvalue really is, or whether, if one tries another assumed eigenfunction, the second approximation is better or worse than the first. We merely wish to point out how little is actually known, in a mathematical sense, about integral equations of this type. We believe that computer-generated numerical solutions, although admittedly laborious, will furnish the most reliable results that we are likely to get from the integral equations of laser theory, at least until someone develops an adequate analytic theory of integral equations with complex symmetric kernels.

The Dipolar Resonance of the Cylindrical Low-Pressure Arc Discharge*

JOSEPH H. BATTOCLETTI†, SENIOR MEMBER, IEEE

Summary—When an em wave of fixed frequency is incident on the cylindrical positive column of a low-pressure arc discharge, nearly complete absorption occurs at a definite value of discharge current I_0 as the discharge current is varied. I_0 yields a plasma electron density which corresponds to the well-known cylindrical, or dipolar, plasma resonance frequency f_0. The ratio f_p/f_0 where f_p is the ordinary (plane) plasma frequency, has been determined by others using a quasi-static approach. In this paper a dynamic approach is used, and comparison is made with the quasi-static approach. Agreement is within 3 per cent for values of $\beta_0 a$ less than 0.25. For $\beta_0 a$ equal to 0.60, the discrepancy in the quasi-static method is 15 per cent.

Theoretical calculations as well as experimental evidence indicate that the electron sheath, which exists on the outside surface of the positive column, plays a significant role in the location of the dipolar plasma resonance.

Application of the results of this paper improve the agreement between theory and experiment for the Plasma Microwave Coupler described by Steier and Kaufman.

* Received June 11, 1962; revised manuscript received February 15, 1963. This work was supported in part by a grant from the National Science Foundation. Part of this work served in partial satisfaction of the requirements for the Ph.D. in Engineering, University of California, Los Angeles; June, 1961.

† Electronic Consultant to the Chilean Universities for the U. S. National Academy of Sciences and the U. S. Agency for International Development, American Embassy, Casilla 13120, Santiago, Chile. On leave from Marquette University, Milwaukee, Wis.

I. INTRODUCTION

WHEN AN EM WAVE of fixed frequency is incident on the cylindrical positive column of a low-pressure mercury-vapor discharge, a spectrum of resonances of reflection and transmission occurs as the discharge current of the positive column is varied. Nearly complete absorption occurs at a definite value of current I_0 which yields a plasma density corresponding to the well-known cylindrical, or dipolar, plasma resonance frequency. If the discharge current is maintained constant, an analogous spectrum of resonances occurs as the frequency of the incident em wave is varied. Nearly complete absorption occurs at a definite value of frequency f_0 which is the dipolar plasma resonance frequency. If the plasma electron density is assumed to be linearly related to the discharge current,

TABLE I

FORMULAS FOR K_{eff} FOR SEVERAL DIFFERENT CASES OF A HETEROGENEOUS CYLINDRICAL MEDIUM SURROUNDING A PLASMA COLUMN. K_e IS THE RELATIVE DIELECTRIC CONSTANT OF THE GLASS TUBE. $R=(K_e-1)/(K_e+1)$.

Case	Media Surrounding Plasma Column	K_{eff}	Reference
I	Free Space	1	[1]
II	1) Glass Tube ID $=2a$, OD $=2b$ 2) Free Space	$K_e \dfrac{1-\left(\frac{a}{b}\right)^2 R}{1+\left(\frac{a}{b}\right)^2 R}$	[2], [3]
III	1) Glass Tube ID $=2a$, OD $=2b$ 2) Free Space 3) Metal Tube ID $=2d$	$K_e \dfrac{\left(\frac{b}{a}\right)^2\left(1-\left(\frac{b}{d}\right)^2 R\right)-\left(R-\left(\frac{b}{d}\right)^2\right)}{\left(\frac{b}{a}\right)^2\left(1-\left(\frac{b}{d}\right)^2 R\right)+\left(R-\left(\frac{b}{d}\right)^2\right)}$	[4]
IV	1) Glass Tube ID $=2a$, OD $=2b$ 2) Metal Tube ID $=2b$	$K_e \dfrac{\left(\frac{b}{a}\right)^2+1}{\left(\frac{b}{a}\right)^2-1}$	

then the relation between I_0 and f_0 is given by

$$I/I_0 = (f_0/f)^2, \tag{1}$$

which is written in terms of a variable discharge current I and a variable signal frequency f.

The dipolar plasma resonance frequency f_0 may be related to the ordinary (plane) plasma frequency f_p and I_0 may be related to I_p, according to the equations

$$f_0 = f_p/(1 + K_{\text{eff}})^{1/2} \tag{2}$$

$$I_0 = I_p(1 + K_{\text{eff}}), \tag{3}$$

where K_{eff} is the *effective* relative dielectric constant of the heterogeneous cylindrical medium surrounding the plasma column. K_{eff} is given in Table I for several different cases.

f_0 is less than f_p (or, equivalently, I_0 is greater than I_p); the effect of the surrounding media is to increase these inequalities.

The formulas for K_{eff} have been derived by using a quasi-static approach, which utilizes the solution of Laplace's equation for a scalar potential that does not vary with time. Boundary conditions involving potential and potential gradient at the interfaces are matched in order to determine the constants of integration of the solution of Laplace's equation, or to obtain a characteristic equation. The solution of the characteristic equation for a resonant condition leads to an equation which is interpreted as follows: the relative dielectric constant of the plasma at resonance is equal to the negative of the *effective* dielectric constant of the heterogeneous medium surrounding the plasma, that is, $\epsilon_{rp} = -K_{\text{eff}}$. From an elementary study [5], [6], the relative dielectric constant of a plasma, neglecting collisions, is given by

$$\epsilon_{rp} = 1 - (f_p/f)^2. \tag{4}$$

The substitution of $(-K_{\text{eff}})$ for ϵ_{rp} in (4) yields the general equation for f_0, namely (2).

When the dynamic approach is used, a wave equation which includes the time variable is solved. Boundary conditions involving electric field intensity and magnetic field intensity at the interfaces are matched in order to obtain a characteristic equation. The characteristic equation has multiple roots which yield not one but a series of natural modes of oscillation of the cylindrical system. The primary root corresponds to the cylindrical, or dipolar, plasma resonance condition.

It is a purpose of this paper to demonstrate the use of the more accurate dynamic approach, and to compare its results with those of the quasi-static approach.

Experimental data are offered regarding the temperature dependence of the cylindrical plasma resonance current, I_0. Physical factors, such as the location of the metal waveguide near the positive column of the discharge tube, temperature distribution axially along the discharge tube, and selective cooling, are treated.

Finally, application of these data is made to the quantitative results described by Steier and Kaufman [4] of a new type of microwave coupler, which uses a gas discharge tube as a coupling device.

II. THE NATURAL MODES OF OSCILLATION OF A CYLINDRICAL PLASMA USING THE DYNAMIC APPROACH

An infinitely long homogeneous cylindrical plasma with a concentric glass tube imbedded in free space is

TABLE II
DESCRIPTION OF A THREE-MEDIUM CONCENTRIC CYLINDRICAL SYSTEM. THE ORIENTATION OF THE SYSTEM IS ALONG THE Z AXIS

Medium	Radius		Permittivity	Permeability	Phase Constant
	Inner	Outer	ϵ	μ	$\beta=\omega(\mu\epsilon)^{1/2}$
Space	b	∞	ϵ_0	μ_0	β_0
Glass	a	b	$\epsilon_g=\epsilon_{rg}\epsilon_0$	μ_0	$\beta_g=(\epsilon_{rg})^{1/2}\beta_0=n_g\beta_0$
Plasma	0	a	$\epsilon_p=\epsilon_{rp}\epsilon_0$	μ_0	$\beta_p=(\epsilon_{rp})^{1/2}\beta_0=n_p\beta_0$

first considered. A characteristic equation is developed for this three-medium system, which, by observation, may be simplified for the simple model of the plasma itself or may be extended for additional concentric layers. The three-medium system is described in Table II.

For a homogeneous charge-free medium (assumed for all models considered here), it is possible to express the electromagnetic field in terms of two independent one-Cartesian-component Hertzian vectors, $\mathbf{\Pi}$ and $\mathbf{\Pi}^*$ [7]. The logical choice for the component in the cylindrical problem is the z direction. For a TE-wave problem (the case we wish to consider), only Π_z^* is needed. The electric and magnetic vector fields, for a common time dependence $e^{-j\omega t}$ are given as:[1]

$$\boldsymbol{E} = j\omega\mu\nabla\times(\mathbf{1}_z\Pi_z^*) \tag{5}$$

$$\boldsymbol{H} = \nabla\nabla\cdot(\mathbf{1}_z\Pi_z^*) - (j\omega)^2\mu\epsilon(\mathbf{1}_z\Pi_z^*). \tag{6}$$

Since this analysis is made for fields independent of the z-axis coordinate, (5) and (6) reduce to:

$$\boldsymbol{E} = j\omega\mu\left(\mathbf{1}_r\frac{1}{r}\frac{\partial\Pi_z^*}{\partial\theta} - \mathbf{1}_\theta\frac{\partial\Pi_z^*}{\partial r}\right) \tag{7}$$

$$\boldsymbol{H} = -\mathbf{1}_z(j\omega)^2\mu\epsilon\Pi_z^*. \tag{8}$$

A restriction to Π_z^* is that it should satisfy the scalar Helmholtz equation $\nabla^2\psi+k^2\psi=0$. Variables in this equation are separated in the conventional manner, and the differential equation involving r only is a Bessel equation. The Π_z^*'s are therefore chosen appropriately, and are given as Fourier-Bessel Series as follows:

$$\Pi_{z(\text{space})}^* = \sum_{n=0}^{\infty} a_nH_n(\beta_0r)\cos n\theta \tag{9}$$

$$\Pi_{z(\text{glass})}^* = \sum_{n=0}^{\infty} (b_nJ_n(\beta_gr) + c_nN_n(\beta_gr))\cos n\theta \tag{10}$$

$$\Pi_{z(\text{plasma})}^* = \sum_{n=0}^{\infty} d_nJ_n(\beta_pr)\cos n\theta. \tag{11}$$

$J_n(x)$ is the Bessel Function of the First Kind, $N_n(x)$ is the Neumann Function, and $H_n(x)$ is the Hankel Function of the First Kind. The field quantities E_r, E_θ, and H_z are obtained by substituting (9), (10), and (11) into (7) and (8).

The tangential components of E_θ and H_z must be continuous across the boundary of adjacent media. In this model there are two such boundaries. Four equations of the coefficients, a_n, b_n, c_n and d_n, are thus obtained. The right-hand sides of the four equations are zero, since there are no terms without the coefficients. The determinant of the set of four equations must therefore be equal to zero for a nontrivial solution. The resulting characteristic equation is given as a fourth-order determinant by

$$\begin{vmatrix} H_n'(\beta_0b) & J_n'(\beta_gb) & N_n'(\beta_gb) & 0 \\ H_n(\beta_0b) & n_gJ_n(\beta_gb) & n_gN_n(\beta_gb) & 0 \\ 0 & J_n'(\beta_ga) & N_n'(\beta_ga) & J_n'(\beta_pa) \\ 0 & n_gJ_n(\beta_ga) & n_gN_n(\beta_ga) & n_pJ_n(\beta_pa) \end{vmatrix} = 0, \tag{12}$$

where n_g and n_p are indexes of refraction of the two non-free-space media, and are equal to $(\epsilon_{rg})^{1/2}$ and $(\epsilon_{rp})^{1/2}$, respectively. The primary root of (12), obtained for $n=1$, yields the condition for the cylindrical, or dipolar, plasma resonance. An exact solution is difficult because of the transcendental nature of (12). However, three approximate methods of solution are illustrated.

Approximation 1

In the most severe approximation, which yields the results of the static approach, each Bessel Function in (12) is replaced by its small argument expansion. The determinant equation (12) may be expanded to give

$$\left(\frac{J_n(\beta_gb)}{J_n(\beta_ga)}\right)\left(\frac{H_n'(\beta_0b)}{H_n(\beta_0b)} - \frac{J_n'(\beta_gb)}{n_gJ_n(\beta_gb)}\right)\cdot\left(\frac{N_n'(\beta_ga)}{n_gN_n(\beta_ga)} - \frac{J_n'(\beta_pa)}{n_pJ_n(\beta_pa)}\right) = \left(\frac{N_n(\beta_gb)}{N_n(\beta_ga)}\right)\left(\frac{H_n'(\beta_0b)}{H_n(\beta_0b)} - \frac{N_n'(\beta_gb)}{n_gN_n(\beta_gb)}\right)\cdot\left(\frac{J_n'(\beta_ga)}{n_gJ_n(\beta_ga)} - \frac{J_n'(\beta_pa)}{n_pJ_n(\beta_pa)}\right). \tag{13}$$

[1] J. A. Stratton [6], p. 31.

The ratios in (13), evaluated by using the small argument expansions of the Bessel Functions, are particularly simple and are:

$$\frac{H_n'(x)}{H_n(x)} \cong \frac{N_n'(x)}{N_n(x)} \cong -\frac{n}{x}; \qquad \frac{J_n'(x)}{J_n(x)} \cong \frac{n}{x};$$
$$\frac{J_n(x)}{J_n(y)} \cong \left(\frac{x}{y}\right); \qquad \frac{N_n(x)}{N_n(y)} \cong \left(\frac{y}{x}\right)^n. \tag{14}$$

y using (14), (13) simplifies to

$$n_p^2 = \epsilon_{rp} = -\epsilon_{rg}\frac{1-\left(\frac{a}{b}\right)^{2n}\frac{\epsilon_{rg}-1}{\epsilon_{rg}+1}}{1+\left(\frac{a}{b}\right)^{2n}\frac{\epsilon_{rg}-1}{\epsilon_{rg}+1}}. \tag{15}$$

For $n=1$, the right-hand side of (15) is equal to $-K_{\text{eff}}$ as given by Case II of Table I. (ϵ_{rg} is the same as K_e.) This approximation is relatively severe, particularly when the arguments, $\beta r = \omega(\epsilon_r)^{1/2}(\epsilon_0\mu_0)^{1/2} r$, of the Bessel Functions are not small.

Approximation 2

When the size of the tube is specified, every element of the determinant equation (12) may be computed exactly, except for the elements in the last column. (β_p, or rather, ϵ_{rp}, is the unknown which we are attempting to determine.) Therefore, (12) may be expressed as

$$J_n'(\beta_p a)/(\beta_p a)J_n(\beta_p a) = \boldsymbol{B}_n, \tag{16}$$

where $\boldsymbol{B}_n$ is given by

$$\boldsymbol{B}_n = -(1/\beta_0 a)(\boldsymbol{\Delta}_{44}/\boldsymbol{\Delta}_{43}). \tag{17}$$

$\boldsymbol{\Delta}$'s are the minors of the determinant. $\boldsymbol{B}_n$ is a complex number with a negative real part and a small positive imaginary part. A small argument expansion, when applied to the left-hand side of (16), yields, for $n=1$,

$$\epsilon_{rp} = -1/|\text{ Real } \boldsymbol{B}_1|\,(\beta_0 a)^2$$
$$= -1/B_{1R}(\beta_0 a)^2, \tag{18}$$

where $|\text{Real } \boldsymbol{B}_1|$, identified as B_{1R} for simplicity, is the magnitude of the real part of the complex quantity, $\boldsymbol{B}_1$. Only the real part of $\boldsymbol{B}_1$ is taken, since the left-hand side of (16) will be real because collisions inside the plasma have not been considered.

Approximation 3

In this approximation, (16) and (17) are used, but the approximation assigned to the left-hand side of (16) is less severe. The first several terms of the power series of $J_n(\beta_p a)$ and its derivative are taken, and terms of the entire left-hand side of (16) up through the fourth power of $(\beta_p a)$ are retained. The resultant equation is

$$\boldsymbol{K}_n(\beta_p a)^4 + \boldsymbol{L}_n(\beta_p a)^2 + \boldsymbol{M}_n = 0. \tag{19}$$

For $n=1$, it is found that $\boldsymbol{K}_1 = (\boldsymbol{B}_1/8 + 5/192)$, $\boldsymbol{L}_1 = -(\boldsymbol{B}_1 + 3/8)$, and $\boldsymbol{M}_1 = 1$. The solution of this quadratic equation yields two roots, only the smaller of which is of interest here. After a binomial expansion is applied to the square root portion, the resulting solution for ϵ_{rp} is

$$\epsilon_{rp} = -\frac{(B_{1R} - 0.0729)}{B_{1R}(B_{1R} + 0.208)} \times \frac{1}{(\beta_0 a)^2}. \tag{20}$$

Again only the real part of $\boldsymbol{B}_1$ is used. Eq. (20) degenerates to the second approximation when $B_{1R} \gg 0.208$.

Several examples of the results of computations of (15), (18) and (20) for different plasma tubes are given in Table III. The frequency ratio f_p/f_0 calculated from (4), is listed rather than ϵ_{rp}. The discrepancy between the quasi-static and dynamic approaches increases as the value of $(\beta_0 a)$ increases. For Case E, the discrepancy is 15 per cent. To obtain a correspondence within 3 per cent, the value of $(\beta_0 a)$ should not exceed approximately 0.25. The correspondence between the solution from (18) and (20) in the dynamic approach is good for values of $(\beta_0 a)$ up to approximately 0.50.

Characteristic equations, in determinant form, are given in Table IV for other plasma models. The cases correspond to those given in Table I. The uniform electron sheath in Case V is considered as another dielectric layer, adjacent to and concentric with the plasma column. n_s is the refractive index (equal to $(\epsilon_{rs}^{1/2})$ of the electron sheath. The density of the sheath is considered to be less than the density of the plasma. The primary root $n=1$ corresponds to the dipolar plasma resonance condition.

III. The Effect of the Electron Sheath on the Modes of Oscillation of a Cylindrical Plasma

The existence of an electron sheath at the outside surface of the positive column of a discharge tube is well known and has been studied experimentally by Gabor [8], [9]. Calculations applied to Gabor's work [10] lead to a sheath thickness of 1/12 of the tube radius, and an electron density less than the electron density of the plasma in the positive column. The lesser electron density causes the dielectric constant of the sheath to be positive and less than the value for free space.

The dynamic approach leads to the characteristic equation of Case V of Table IV. One possible expansion yields

$$\frac{J_n'(\beta_p c)}{(\beta_p c)J_n(\beta_p c)} = \frac{1}{(\beta_s c)}\left[\frac{N_n'(\beta_s c) - J_n'(\beta_s c)\left(\frac{(\beta_s a)\boldsymbol{B}_n N_n(\beta_s a) - N_n'(\beta_s a)}{(\beta_s a)\boldsymbol{B}_n J_n(\beta_s a) - J_n'(\beta_s a)}\right)}{N_n(\beta_s c) - J_n(\beta_s c)\left(\begin{array}{c}\text{Same as expression in}\\ \text{above parenthesis}\end{array}\right)}\right], \tag{21}$$

TABLE III

COMPARISON OF f_p/f_0 AS DETERMINED FOR DIFFERENT PLASMA TUBES, USING THE QUASI-STATIC AND DYNAMIC APPROACHES, FOR THE MODEL OF TABLE II

Case	b/a	f in Mc	$\beta_0 a$	$f_p/f_0=(1-\epsilon_{rp})^{1/2}$		
				Static Eq. (15)	Dynamic Eq. (18)	Dynamic Eq. (20)
A	2.66	4400	0.1037	2.05	2.08	2.09
B	1.82	4400	0.126	1.91	1.93	1.94
C	1.27	4400	0.253	1.67	1.71	1.72
D	1.40	7050	0.370	1.75	1.83	1.86
E	1.40	12000	0.628	1.75	1.88	2.07
The following Case F is the same as Case E, except a 10 mm ID metal tube has been added. Also, the formula of Case III, Table I, is used instead of (16).						
F	1.40	12000	0.628	2.08	Not Determinable	

TABLE IV

CHARACTERISTIC EQUATIONS, IN DETERMINANT FORM, FOR DIFFERENT PLASMA MODELS. THE CASES CORRESPOND TO THOSE OF TABLE I

Case	Media Surrounding Plasma Column	Characteristic Equation
I	Free Space Plasma Column = radius a	$\begin{vmatrix} H_n'(\beta_0 a) & J_n'(\beta_p a) \\ H_n(\beta_0 a) & n_p J_n(\beta_p a) \end{vmatrix} = 0$
II	1) Glass Tube, ID $=2a$, OD $=2b$ 2) Free Space	See Equation (12)
III	1) Glass Tube, ID $=2a$, OD $=2b$ 2) Free Space 3) Metal Tube, ID $=2d$	$\begin{vmatrix} J_n'(\beta_0 d) & N_n'(\beta_0 d) & 0 & 0 & 0 \\ J_n'(\beta_0 b) & N_n'(\beta_0 b) & J_n'(\beta_g b) & N_n'(\beta_g b) & 0 \\ J_n(\beta_0 b) & N_n(\beta_0 b) & n_g J_n(\beta_g b) & n_g N_n(\beta_g b) & 0 \\ 0 & 0 & J_n'(\beta_g a) & N_n'(\beta_g a) & J_n'(\beta_p a) \\ 0 & 0 & n_g J_n(\beta_g a) & n_g N_n(\beta_0 a) & n_p J_n(\beta_p a) \end{vmatrix} = 0$
IV	1) Glass Tube, ID $=2a$, OD $=2b$ 2) Metal Tube, ID $=2b$	$\begin{vmatrix} J_n'(\beta_g b) & N_n'(\beta_g b) & 0 \\ J_n'(\beta_g a) & N_n'(\beta_g a) & J_n'(\beta_p a) \\ n_g J_n(\beta_g a) & n_g N_n(\beta_g a) & n_p J_n(\beta_p a) \end{vmatrix} = 0$
V	1) Sheath, ID $=2c$, OD $=2a$ 2) Glass Tube, ID $=2a$, OD $=2b$ 3) Free Space	$\begin{vmatrix} H_n'(\beta_0 b) & J_n'(\beta_g b) & N_n'(\beta_g b) & 0 & 0 & 0 \\ H_n(\beta_0 b) & n_g J_n(\beta_g b) & n_g N_n(\beta_g b) & 0 & 0 & 0 \\ 0 & J_n'(\beta_g a) & N_n'(\beta_g a) & J_n'(\beta_s a) & N_n'(\beta_s a) & 0 \\ 0 & n_g J_n(\beta_g a) & n_g N_n(\beta_g a) & n_s J_n(\beta_s a) & n_s N_n(\beta_s a) & 0 \\ 0 & 0 & 0 & J_n'(\beta_s c) & N_n'(\beta_s c) & J_n'(\beta_p c) \\ 0 & 0 & 0 & n_s J_n(\beta_s c) & n_s N_n(\beta_s c) & n_p J_n(\beta_p c) \end{vmatrix} = 0$

where B_n is given by (17). The condition for the dipolar mode of oscillation occurs for $n=1$.

Generalization of the results of (21) is difficult if not impossible. Therefore, calculations are made for a typical discharge tube at a particular signal frequency, namely, $a=2.5$ mm, $b=3.5$ mm, and $f=12{,}000$ Mc. Values of f_p/f_0 as a function of the sheath thickness $t=a-c$ for several values of sheath electron density N_s are plotted in Fig. 1. The points have been calculated using the method of Approximation 3 of Section II. For the case of no sheath, that is, for the condition of Case E in Table III, f_p/f_0 is equal to 2.07. For the case of the sheath, whose density is less than the plasma density, f_p/f_0 is always less than 2.07 and may be appreciably less when the density of the sheath approaches the density of the plasma. When the electron sheath density N_s corresponds to the ordinary plasma frequency, that is, $f_s=f_p$, the effective dielectric constant of the material surrounding the plasma is zero, and the cylindrical plasma frequency f_0 is equal to the ordinary plasma frequency f_p. The effect of the sheath, therefore, has been to decrease the *effective* dielectric constant K_{eff} of the material surrounding the plasma; f_0 thus increases and I_0 decreases.

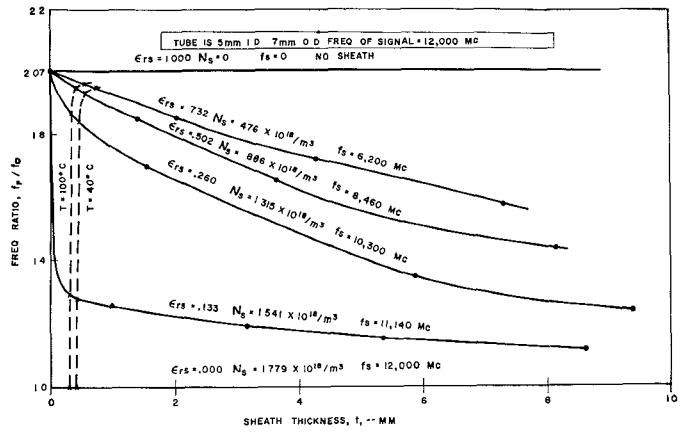

Fig. 1—Theoretical variation of the frequency ratio f_p/f_0 vs sheath thickness and sheath density.

In order to obtain additional information concerning the thickness and density of the sheath, it is necessary at this point to consider the physical phenomena taking place inside the positive column of the arc discharge. Klarfeld [11] has obtained a theoretical curve of electron temperature as a function of Rp_0, where R is the radius of the positive column and p_0 is the vapor pressure of the mercury reduced to 0°C. In addition, an equation for the potential drop across the electron sheath has been derived [12], and is

$$\Delta V = (kT_e/2e) \ln (T_e m_p / T_p m_e)$$
$$= 4.308 \times 10^{-5} T_e (12.809 + \ln T_e - \ln T_p), \quad (22)$$

where T_e and T_p are the random motion temperatures, and m_e and m_p are the masses, of the electrons and positive ions, respectively. The temperature of the positive ions is approximately equal to the temperature of the gas. In fact, for calculation purposes in (22), the temperature which determines the vapor pressure of the mercury may be used for T_p with good accuracy.

An electrostatic approach to the analysis of the electron sheath yields an equation for the product of the sheath density and the square of the sheath thickness [10]. Application of Gauss's Law to determine the electric flux density in the sheath and the use of the potential integral

$$\Delta V = \int_c^a \boldsymbol{E} \cdot d\boldsymbol{l}$$

yields, for $t \ll a$,

$$\Delta V = N_s e t^2 / 2\epsilon_0 = 9.047 \times 10^{-9} N_s t^2. \quad (23)$$

ΔV may be eliminated in (23) by the substitution of (22); the explicit equation for t is, therefore,

$$t = 69.007 (T_e/N_s)^{1/2} (12.809 + \ln T_e - \ln T_p)^{1/2}. \quad (24)$$

When calculations are carried out at mercury-pool temperatures of 100°C and 40°C, the dashed curves of Fig. 1 are obtained. For example, at 100°C and $N_s = 1.779 \times 10^{18}$, $p = 0.25$ mm Hg, $Rp_0 = 0.045$ for $R = 2.5$ mm, $T_e = 18{,}300$°K, $\Delta V = 13.2$ volts, and $t = 0.0286$ mm. Over most of the range of sheath electron density, the thickness of the sheath is between 0.03 and 0.04 mm (1/80 to 1/60 of the radius of the tube) for the temperature range selected.

IV. Experimental Results

A. Temperature Dependence of the Cylindrical Plasma Resonance Discharge Current I_0

It has been shown experimentally [10], [13] that the discharge current required to obtain the cylindrical plasma resonance from the positive column of a mercury arc discharge for an em wave of fixed frequency, is dependent on the operating temperature of the positive column (the temperature of the neutral mercury atoms). This temperature is determined by ohmic losses inside the positive column as well as by the ambient temperature. The variation of the resonance current I_0 as a function of ambient temperature is plotted as the solid curve in Fig. 2 for a mercury-pool type discharge tube. The trend is seen to be a decreasing value of I_0 as temperature is increased, due in part to an increasing percentage of ionization. The values of I_0 were obtained dynamically by sweeping the discharge current at a 60-cycle rate, so that the complete resonance spectrum, including several of the lesser resonances (see, for example, Figs. 4 and 5), could be obtained visually. The temperature of the mercury pool, which governs the vapor pressure, has a lesser effect on the location of I_0 than the temperature of the positive column. The dashed curve of Fig. 2, which illustrates the variation of I_0 as a function of the ambient temperature of the positive column alone, generally follows the solid curve. It is therefore probable that the electron sheath of the positive column plays a major role in the determination of the value of I_0.

Temperature variations exist along the axis of the positive column of the plasma tube. In fact, the temperature at the high-voltage anode end of the tube may

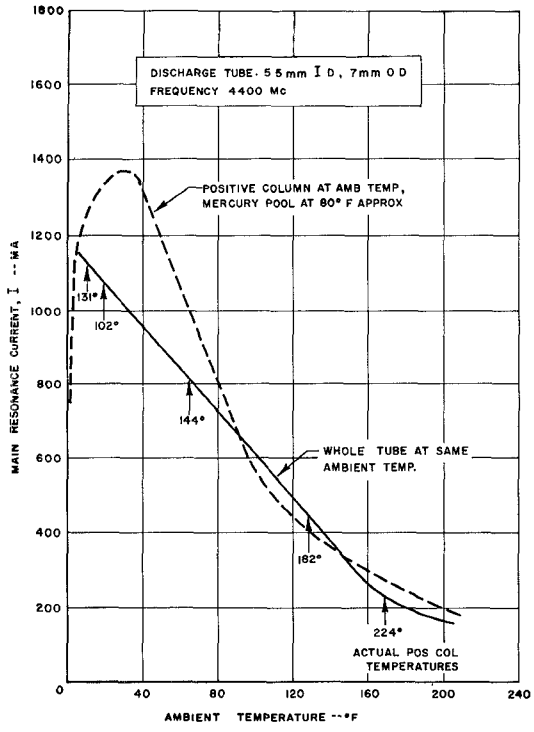

Fig. 2—Main resonance current I_0 vs ambient temperature.

be appreciably higher than the temperature at the middle portion of the tube, due principally to anode dissipation. The degree of ionization and the electron density are therefore larger at the anode end of the tube. This temperature difference may be verified by the use of thermocouples, but a more interesting comparison is obtained by setting up the waveguide circuit of Fig. 3. A double resonance spectrum is thus obtained, one spectrum from the central portion of the tube, and one spectrum from a portion near the anode. The photographs of Fig. 4 demonstrate the difference between the values of I_0, and show how this difference is a function of the distance a (see Fig. 3), that is, the difference of the temperature of the two parts of the plasma tube. Fig. 4(a) illustrates that the value of I_0 is greater in the central part of the plasma tube than it is near the anode end and that the value of I_0 for the anode-end waveguide decreases as the waveguide is brought near to the anode end. The data are presented in Table V. The effect will be more pronounced for X band than for S band, since the amount of plasma tube inside the X-band waveguide is less, and thus the X-band waveguide can be located closer (on the average) to the anode end. Indeed, a typical experiment at X band has given a much greater difference (see Table V).

Fig. 4(b) illustrates that selective cooling of the two parts of the plasma tube can vary the value of I_0 of each part. The data are also presented in Table V. The cooling was accomplished by two small blowers, one for each part of the tube. A baffle was placed between the two waveguides to allow only one portion of the tube to receive the cooling stream of air. Even so, there is some interaction between the two parts of the plasma tube.

B. The Effect of Waveguide Metal on the Plasma Resonance Discharge Current I_0

Many of the experimental setups used in studying microwave interactions with plasmas require the positive column of the plasma tube to be in proximity to the top and bottom walls of the waveguide. Cases III and IV of Table I, which have been derived using the static approach, and Cases III and IV of Table IV, which have been derived using the dynamic approach, would predict that the metal will have an effect on the location of the cylindrical plasma resonance (see Cases E and F, Table III). However, the prediction is not supported by experiment.

The ordinary S-band waveguide No. 2 of Fig. 3 was replaced with one in which the small dimension was decreased to 11 mm (see the insert of Fig. 3). Thus, the waveguide top and bottom walls were close to the plasma tube. The photographs of Fig. 5 demonstrate the same effects of Fig. 4, but for the constricted waveguide. The results are essentially the same. The conclusion to be reached from these data is that the constriction in the waveguide, which brought metal close to the plasma tube, did not essentially change the values of I_0 nor the separation between the values of I_0 for the two waveguides. It may be conjectured, therefore, that the electron sheath has a predominant effect on the value of I_0 and tends to shield the plasma from the metal waveguide.

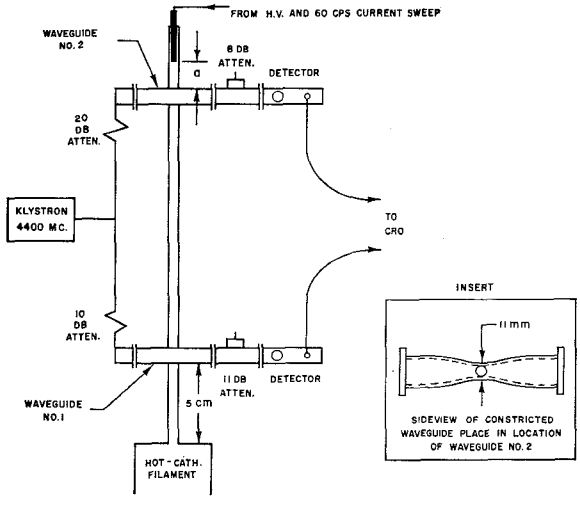

Fig. 3—Diagram of the experimental setup used to obtain the photographs of Fig. 4 and Fig. 5.

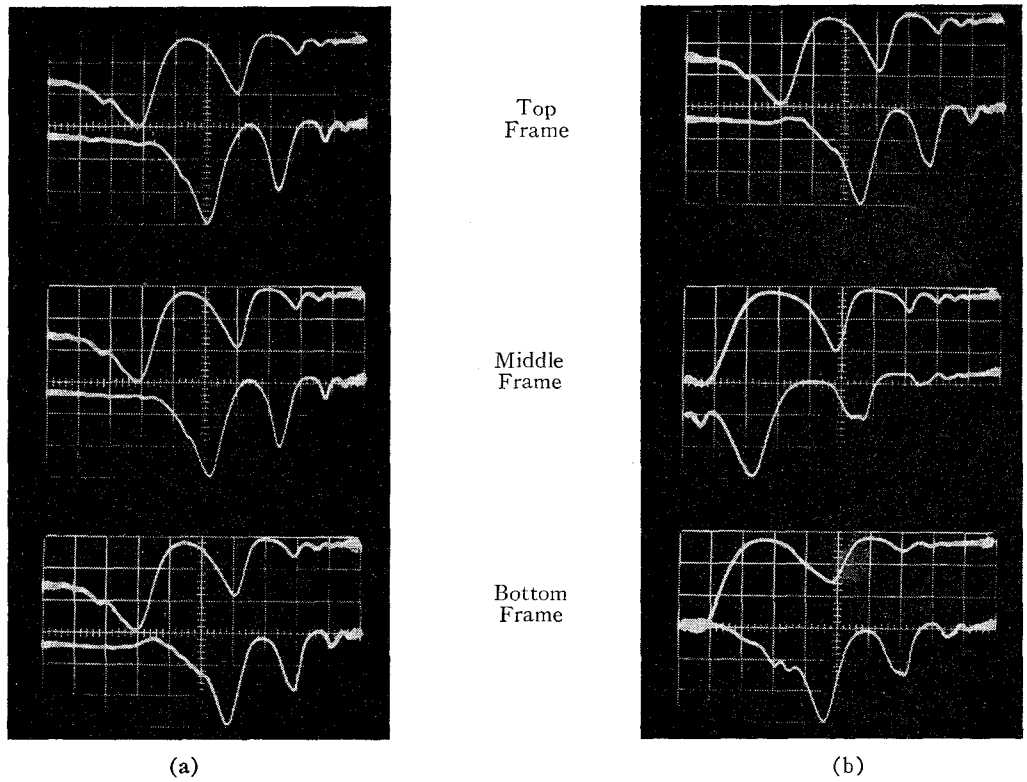

Fig. 4—Oscillograms of resonance spectra obtained from the setup of Fig. 3. The bottom spectrum of each frame was obtained from the waveguide near the anode. Current increases to the left; the current at the center is 360 Ma, and the current scale is 10 Ma per small division. The vertical scale is proportional to the power transmitted past the plasma tube. Cutoff occurs at the bottom of each of the main resonance dips. (a) Variation of distance *a*. (b) Variation of temperature. See Table V for specific details.

TABLE V

DATA FROM FIG. 4 WHICH ILLUSTRATE THE EFFECT OF VARIATIONS OF TEMPERATURE ALONG THE AXIS OF THE POSITIVE COLUMN OF A DISCHARGE TUBE

Photograph Fig.	Value of I_0 (Ma)		Difference in I_0 (Ma)
	Middle Waveguide (No. 1)	Anode End Waveguide (No. 2)	
Fig. 4(a) (No cooling)			
Top Frame, $a=3$ cm	470	360	110
Middle Frame, $a=1$ cm	467	355	112
Bottom Frame, $a=-\frac{1}{2}$ cm	462	320	142
Fig. 4(b) ($a=-\frac{1}{2}$ cm)			
Top Frame: No Cooling	460	335	125
Middle Frame: Anode End Cooled	580	500	80
Bottom Frame: End and Middle Cooled	580	380	200
X-Band Test	1725	1020	705

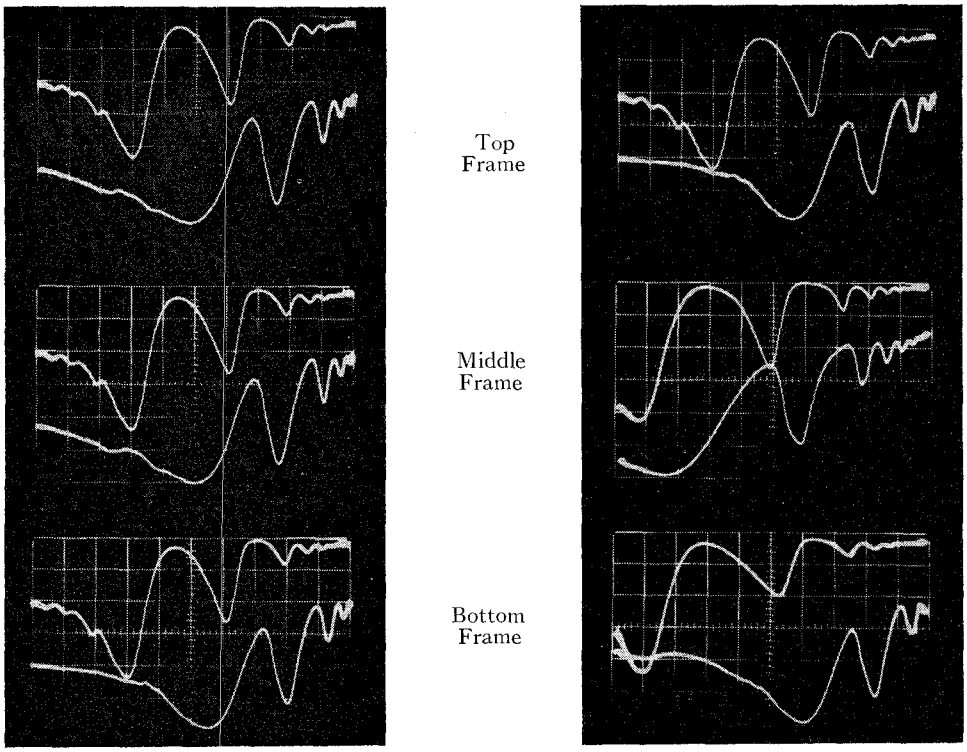

Fig. 5—Oscillograms of resonance spectrum obtained from the setup of Fig. 3 using the constricted waveguide at the anode end. Conditions are the same as in Fig. 4. (a) Variation of distance a. (b) Variation of temperature See Table V for specific details.

V. Remarks About a Plasma Guide Microwave Selective Coupler

A new type of microwave coupler has been described by Steier and Kaufman [4], in which a gas discharge tube is passed through two rectangular waveguides that are parallel but are separated by some distance. Propagation along the plasma column between the two waveguides is assumed to occur as a space-charge wave in a mode which has a cutoff frequency given by

$$f = f_p/(1 + K_e)^{1/2}. \tag{25}$$

Eq. (25) is plotted for $K_e = 3.78$ in Fig. 6 as the solid curve. Steier and Kaufman performed experiments at X band, which yielded data, the average of which is plotted in Fig. 6 as the dashed curve.

It should be mentioned, however, that the experimental curve is not entirely experimental, but is based upon an experimental measurement and upon a calculation from theory as follows:

1) A third waveguide was placed near the anode end of the discharge tube (see Fig. 5 of Steier and Kaufman[2]) in order to determine the dipolar plasma frequency f_0 (which they called f_{T-D}, after Tonks and Dattner).

2) The *effective* dielectric constant K_{eff} of the plasma tube in this third waveguide was calculated from theory using a geometric mean between the values computed from Cases II and III of Table I of this paper.

3) The value of f_p was then calculated from (2), namely, $f_0 = f_{T-D} = f_p/(1+K_{\text{eff}})^{1/2}$.

Although there is a large discrepancy between their calculated and observed cutoff curves, they conclude that the correlation is sufficient to verify the mode of operation of the plasma guide coupler. The author would like to offer some corrections to the above measurement and calculation based upon the contents of this paper which will contribute to a decrease of this large discrepancy.

With reference to 1) above, it is likely that the temperature, the per cent ionization, and thus the electron density of the anode-end portion of the positive column was significantly higher than that part of the plasma tube acting in the coupler. Therefore, the value of f_0 which elicited the dipolar resonance was larger than it would have been if the measurement had been made near the center part of the positive column. The data of Fig. 4, which are given in Table V, are used for this situation. Since frequency is proportional to the square root of the current [see (1)] the correction for f_p as calculated from (25) is $(320/462)^{1/2} \times 100$ per cent $= 83$ per cent. (The X-band data of Table V yield a correction of 77 per cent.)

With reference to 2) above, the data of Figs. 4 and 5 (see Section IV-B) illustrate that the waveguide metal has very little effect on the location of the dipolar resonance. Therefore, only Case II of Table I should be used to calculate K_{eff}. For the discharge tube with ID = 5 mm and OD = 7 mm, and for a metal tube with ID = 10 mm, the static data of Table III, Cases E and F, apply. The geometric mean is calculated to be $(1.75 \times 2.08)^{1/2} = 1.91$. The correction in f_p is therefore $1.75/1.91 \times 100$ per cent $= 92$ per cent.

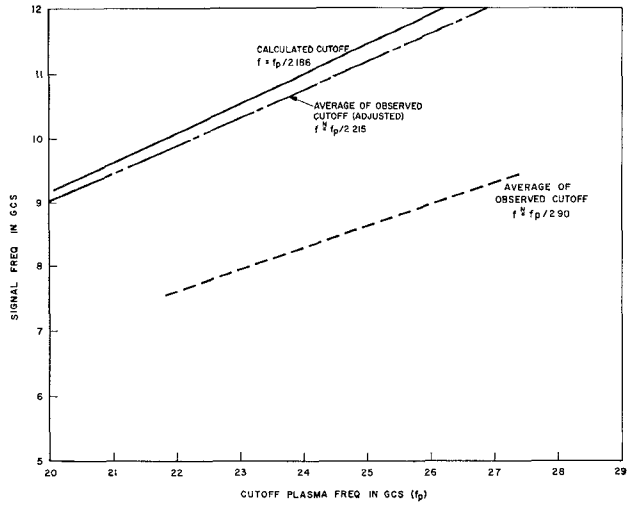

Fig. 6—Signal frequency of the coupler vs cutoff plasma frequency, calculated and experimental (after Steier and Kaufman [4]). The adjusted curve is computed in this paper.

An adjusted experimental curve, taking the temperature dependence of f_0 and the noneffect of waveguide metal on the calculation of K_{eff} into account, is plotted along with the calculated cutoff curve and the average observed cutoff curve in Fig. 6. The total correction is $0.83 \times 0.92 \times 100$ per cent $= 76.5$ per cent. There is now a much closer correspondence between theory and experiment with these two corrections.

Although the two corrections to the work of Steier and Kaufman give a closer correspondence between their theory and experiment, two other considerations must be taken into account in order to give a complete analysis of this problem. The two considerations are:

1) The dynamic approach vs the static approach is discussed in Section II and is summarized in Table III. Case E is of interest here. The correction to the experimental curve of Fig. 6, which is obtained when the dynamic approach is used to compute f_p, is $2.07/1.75 \times 100$ per cent $= 118$ per cent. This would cause the experimental curve of Fig. 6 to lie farther away from the calculated curve.

2) However, when the sheath is taken into account, f_p/f_0 may be significantly smaller than 2.07. In fact, the value of f_p/f_0 may be significantly less than the value of 1.75 used to obtain the partial correction of 92 per cent. Fig. 1 indicates that operation lies somewhere in the region of the two dashed curves, but the actual value cannot be determined with the information available at this time.

[2] See [4], p. 503.

VI. Conclusions

One of the purposes of this paper has been to offer a dynamic approach to the theoretical determination of the well-known cylindrical, or dipolar, plasma resonance frequency. Computations illustrate (see Table III) that there is agreement within 3 per cent between the dynamic and quasi-static approaches when the value of $\beta_0 a$ does not exceed 0.25. It is shown that a small-argument expansion of the Bessel Functions in the dynamic approach yields the quasi-static solution.

The electron sheath, which exists on the outside surface of the positive column, is believed to contribute significantly to the location of the dipolar plasma resonance. Several reasons for this belief are:

1) The value of I_0, which yields resonance, is affected to a much greater degree by the temperature of the positive column than by the temperature of the mercury-pool (which governs the vapor pressure). See Fig. 2.

2) Selective cooling of a portion of the positive column affects the value of I_0 of that portion to a greater degree than the other parts of the positive column. See Fig. 4 and Table V.

3) Experiment indicates that the electron sheath has a shielding effect between the plasma and the metal waveguide in the experimental setup. Compare Fig. 4 and Fig. 5, and see Table V.

4) The theoretical calculations (see Fig. 1) indicate that the ratio f_p/f_0 depends upon the electron sheath density and thickness.

The correspondence between theory and experiment of the Plasma Guide Microwave Selective Coupler of Steier and Kaufman has been improved considerably by taking into account a) the temperature dependence of I_0 along the axis of the discharge tube, and b) the noneffect of waveguide metal on the calculation of K_{eff} (or f_p). However, a complete theoretical determination of f_p is not possible without information regarding the density and thickness of the sheath. This information is not available at this time.

VII. Acknowledgment

The author is indebted to Dr. W. D. Hershberger, Professor of Engineering, University of California, Los Angeles, for his assistance and encouragement. He is also indebted to U.C.L.A. for the opportunity to perform post-doctoral experiments which yielded Figs. 2, 4, and 5, and for the preparation of the illustrations. Finally, appreciation is extended to Loyola University of Los Angeles for its generosity in allowing the author to spend one day a week in the pursuit of post-doctoral work in plasmas.

References

[1] L. Tonks, "Plasma-electron resonance, plasma resonance and plasma shape," *Phys. Rev.*, vol. 38, pp. 1219–1223; June, 1941.
[2] R. W. Gould, "Experiments on plasma oscillations," *Proc. Linde Conf. on Plasma Oscillations*, Spencer, Ind., June 8–10, 1959; pp. 167–204.
[3] R. W. Gould, "Study IV, Scattering from a Plasma Column," Plasma Interaction Research Project, California Institute of Technology, December, 1958 to December, 1959, Final Rept.; pp. 12–26.
[4] W. H. Steier and I. Kaufman, "A plasma guide microwave selective coupler," IRE Trans. on Microwave Theory and Techniques, vol. MTT-9, pp. 499–506; November, 1961.
[5] H. H. Skilling, "Fundamentals of Electric Waves," John Wiley and Sons, Inc., New York, N. Y.; p. 238, 1948.
[6] J. A. Stratton, "Electromagnetic Theory," McGraw-Hill Book Co., Inc., New York, N. Y.; p. 327, 1941.
[7] J. R. Mentzer, "Scattering and Diffraction of Radio Waves," Pergamon Press, Inc., New York, N. Y.; ch. 3, 1955.
[8] D. Gabor, E. A. Ash, and E. D. Dracott, "Langmuir's paradox," *Nature*, vol. 176, pp. 916–919; 1955.
[9] E. Gordon, "Microwave Gaseous Discharge: Plasma Oscillations," Research Lab. of Electronics, M.I.T., Cambridge, Mass., Quarterly Progress Rept., pp. 7–10; January 15, 1957.
[10] J. H. Battocletti, "Resonances in the Positive Column of a Low Pressure Arc Discharge," Ph.D. dissertation, Dept. of Engineering, University of California, Los Angeles; June, 1961.
[11] B. Klarfeld, "Characteristics of the positive column of gaseous discharge," *J. Phys., U.S.S.R.*, vol. 5: 2–3, pp. 155–175; 1941.
[12] L. B. Loeb, "Basic Processes of Gaseous Electronics," University of California Press, Berkeley; pp. 337–338, 1960.
[13] J. H. Battocletti and W. D. Hershberger, "Resonances in the positive column of a low-pressure arc discharge," *J. Appl. Phys.*, vol. 33, pp. 2618–2624;; August, 1962.

Correction

Jesse J. Taub, author of "A New Technique for Multimode Power Measurement," which appeared on pages 496–505 of the November, 1962, issue of these Transactions, has called the following to the attention of the *Editor*.

On page 496, the asterisk footnote should have included the following sentence. "This work was supported by the Rome Air Development Center, Griffiss Air Force Base, N. Y., under Contract No AF30(602)-2511."

On page 500, line 10 of Section IV-C, the word "even" should be "odd."